Quarterly Report

Date of report: October 11, 2007

For quarter ending: September 30, 2007

Agreement number: DTPH56-06-X-000029

Agreement Time period: June 30, 2006 to June 29, 2008

Project: Mechanical Properties and Crack Behavior in Line Pipe Steels

Prepared by: NIST, Materials Reliability Division

Project Tasks:
Task 1: Fatigue crack growth
Task 2: Hydrogen charged fatigue crack growth
Task 3: CTOA testing and modeling
Task 4: Fracture surface examination
Task 5: Method for determination of yield strength in high strength pipeline steels and welds
Task 6: Other tasks as assigned
Task 7: Reporting

NIST-Boulder received the contract for this program in early June 2006. Our efforts are focused on CTOA testing of pipeline steels, weldments and heat affected zones (girth and seam), and the development of a model for our dynamic ductile fracture experiments. Last quarter, we have improved on the dynamic version of the CTOA test system by introducing a spring loaded fixture to better simulate the actual velocity of a running crack in a pipeline. This new setup generates a running crack in the pipeline steel specimen at a rate of approximately 5 m/s. While nowhere near as fast as we were hoping, it is still about 6 orders of magnitude faster than conventional quasi-static CTOA testing. Full-thickness fatigue experiments are also under way and the hydrogen charged tests are coming to completion.

The following task updates should be appended to previously submitted quarterly reports.

Technical status of tasks:

Task 1: Fatigue crack growth

The axial fatigue tests continue at r=0.1 and 0.4. The axial specimen (M(T) geometry) testing is almost complete and we plan to finish this portion of the effort early the next quarter. The uneven fatigue crack propagation through the pipe wall thickness in a couple of the specimens has prompted us to investigate this phenomenon further. We have ordered software that will allow us to monitor and record the fatigue crack growth on both the ID and the OD of the pipe wall, enabling us to better understand this uneven crack growth. The software arrived late (at the end of this quarter) and we expect to continue the fatigue testing very early the next quarter. These tests were machined such that fatigue data was generated in only the transverse (circumferential) direction. We machined pipeline specimens in the compact tension (C(T)) geometry for longitudinal crack fatigue testing and have started those tests. They should be complete late this quarter. Initial C(T) specimen were machined and tested in the transverse direction in order to verify data in the different geometry with the axial M(T) fatigue specimens.

In addition to the experimental work described above, a model is being developed that can help describe the influence of the pipe curvature on fatigue properties. This work, described below, will continue into the next 2 quarters and will be reported on as progress warrants.

Fatigue Modelling

To examine the fatigue crack growth rates within the different grades of pipeline steel, full-thickness fatigue specimens (100 mm wide X 600 mm long test section) were machined from the pipe sections. Because flattening the pipe changes the material behavior, curved pipe sections (removed from the as-received pipe) were used for the test specimens. However, most standard test methods are based on flat specimens. Therefore, it was necessary to examine the influence the pipe curvature had on the fatigue crack growth rates. Finite element models of the different pipe geometries were created along with representative flat models of the same pipe; Figure 1 shows these finite element models.

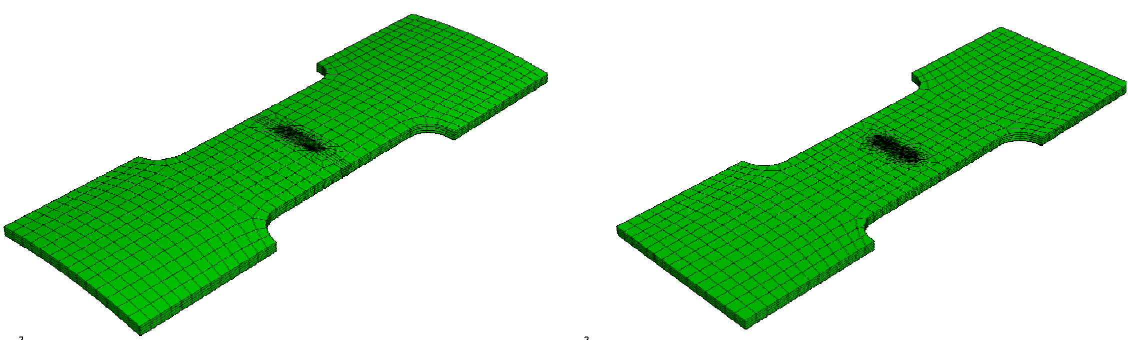

Figure 1. FE Model of (a) curved and (b) flat M(T) specimen with 20 mm crack.

For the analysis, the crack mouth opening displacement on both the outer (OD) and inner (ID) surfaces of the curved model were measured for crack lengths between 8 mm and 36 mm. These were then compared to the results from the flat model and the predicted crack lengths predicted the ASTM E647-05 and the Eftis and Liebowitz crack length-compliance relationships. Figure 2 shows the comparison of the finite element results for an API X65 pipeline steel.

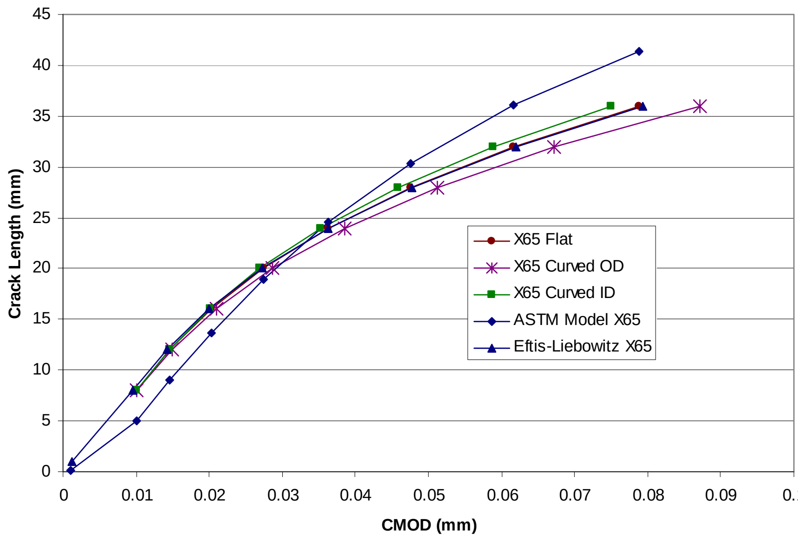

Figure 2. Comparison of FE OD, ID, and Flat results to analytic predictions of crack length.

As can be seen in the figure, the ASTM analytical expression initially under predicts and then significantly over predicts the crack length compared to the three finite element predictions (OD, ID, and Flat). However, the Eftis and Liebowitz expression almost exactly predicts the crack length of the flat model. Therefore to be able to adapt the Eftiz and Liebowitz expression to predict the crack length in the curved model, a correction factor that relates the finite element results for the OD to the results for the flat model is currently being developed. This will then enable the fatigue crack growth test results to be corrected to account for the curvature of the M(T) specimen.

X100 GIRTH WELD MATERIAL PROPERTIES: To better understand the fracture properties (dynamic and quasi-static) of the high strength pipeline steels, we needed reference data on the base metal, heat-affected zone and weld metal interactions.

API X100 high strength grade pipeline steel (outside diameter 52 inch (1.32 m) and wall thickness 20.6 mm) was investigated. Table A contains the nominal chemical composition of this steel (weight %).

Table A Chemical composition of the X100 tested steel (weight %)

C	Mn	P	S	Si	Ni	Cu	Mo
0.07	1.90	0.008	0.0005	0.10	0.50	0.30	0.15

To measure the tensile properties of the pipeline base metal, weld and HAZ, round tensile specimens were machined in both axial (longitudinal) and transverse orientations.

The girth weld was made by use of the shielded metal arc (manual) process for the fill and cap. The root welding electrodes are not specified here.

To characterize the weld section, micro hardness measurements and tensile tests were performed throughout the weld section. Round tensile specimens were machined in the axial (longitudinal) direction, across the weld, with the girth weld and HAZ included in the gauge length (see Fig. 3). An extensometer was used to measure the global elongation of the weld and the two HAZ, and a strain gauge was used to measure the local deformation of the weld.

All experiments were performed in either a screw-driven tensile testing machine of 100 kN capacity, or a closed-loop servo-hydraulic machine of 100 kN capacity. Tests were conducted in displacement control at a rate of 0.1 mm/min.

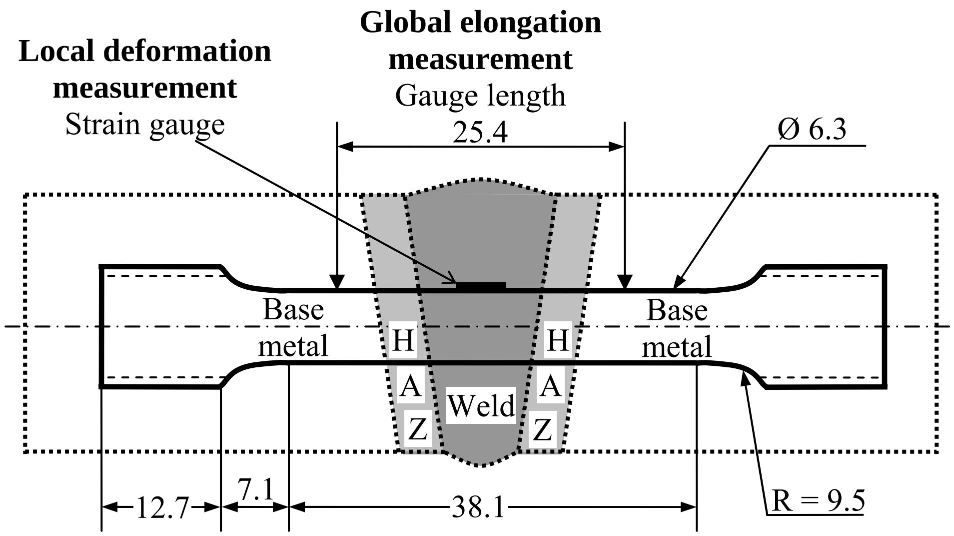

Fig. 3 Round tensile specimen across the girth weld section (dimensions in mm).

A summary of the tensile properties of the base metal and the weld is shown in Table B, where $\sigma_{0.2}$ is the yield stress, σ_{UTS} is the ultimate strength, e_u is the uniform elongation, and e_f is the failure elongation.

Table B Tensile mechanical properties of the base metal and the girth weld

Orientation	$\sigma_{0.2}$ (MPa)	σ_{UTS} (MPa)	$\sigma_{0.2}/\sigma_{UTS}$	e_u (%)	e_f (%)	e_u/e_f
Base Metal Transverse	798	827	0.97	4.1	19.3	0.21
Base Metal Longitudinal	732	806	0.91	4.6	20.3	0.23
Global Girth Weld	602	717	0.84	3.9	11.4	0.35

Fig. 4 presents the tensile test results for the base metal, longitudinal and transverse directions, and for the girth weld (global (weld plus HAZ) and local (weld only)).

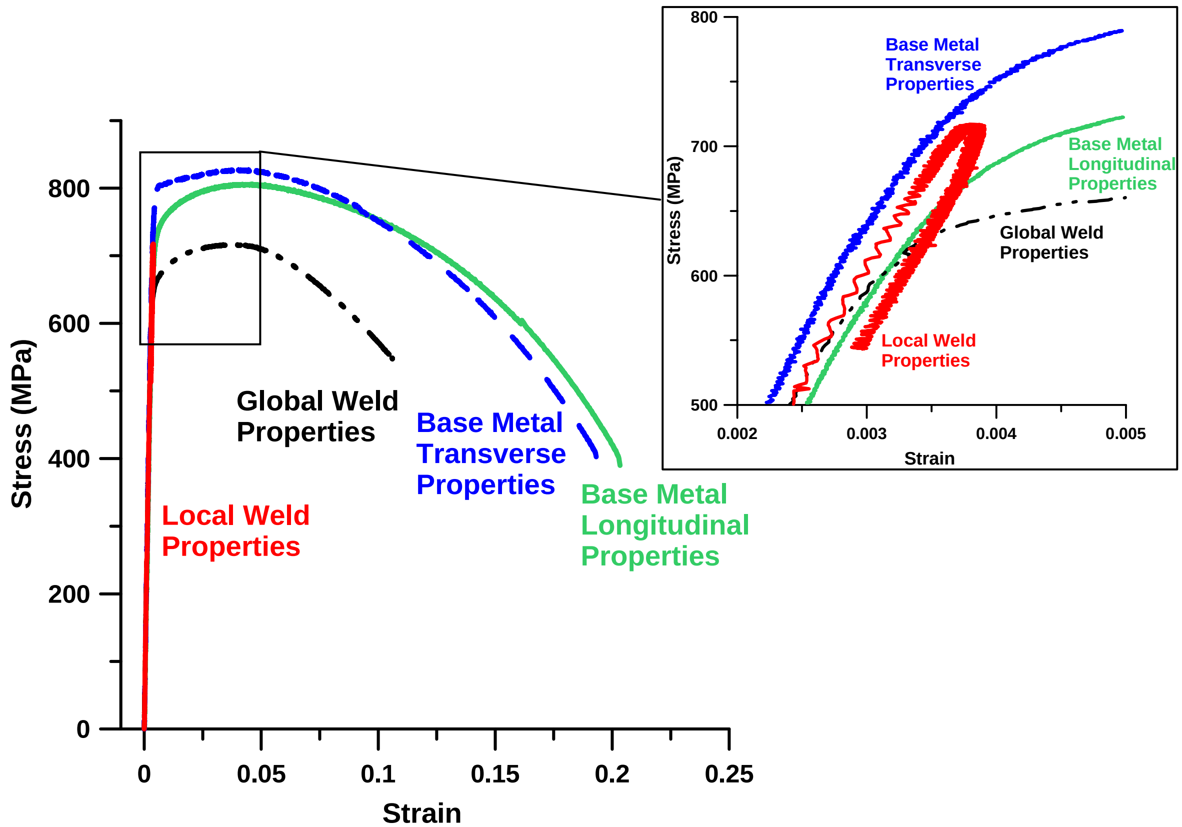

Fig. 4 Base metal and girth weld tensile properties, with details for initial yielding (0.002 to 0.005 strain) shown in the expanded section.

From the tensile tests, several remarks can be made:

- The transverse orientation base metal specimens have a higher yield stress and lower uniform and failure elongation than those for the longitudinal orientation. This result is typical of the pipeline UOE (U-shape, O-shape and Extension) forming process.
- The global girth weld data undermatches the base metal UTS, uniform elongation, and elongation to failure by 11.0 %, 15.2 % and 43.8 %, respectively. These results indicate that this manual weld is not slightly stronger (overmatched) than the base metal, as desired for pipeline service, when a large global deformation is anticipated.
- The weld (local strain measurement) is overmatched in comparison to both the global weld properties (combination of the weld and HAZ sections) and the base metal in the longitudinal direction. Unfortunately, the overmatching can not be quantified by the present tensile test technique because the strain is reduced in the weld section after reaching the UTS because of the necking (localized strain) that occurs in the HAZ near the interface of the HAZ and the base metal.

The mismatch between the weld and HAZ can be quantified by micro hardness measurements. Vickers micro hardness measurements, using a 500 g weight and a diamond point, are presented in Table C and Fig. 5. The hardness measurement indicated a weld overmatch of 4 % and a 10 % under match in the HAZ.

Table C Vickers micro hardness measurements of the girth weld section

Orientation	**Vickers micro hardness measurements, using a 500 g weight and a diamond point**
Base Metal Mean	272
Base Metal Standard Deviation	22
HAZ Mean	244
HAZ Standard Deviation	28
Girth Weld Mean	282
Girth Weld Standard Deviation	24

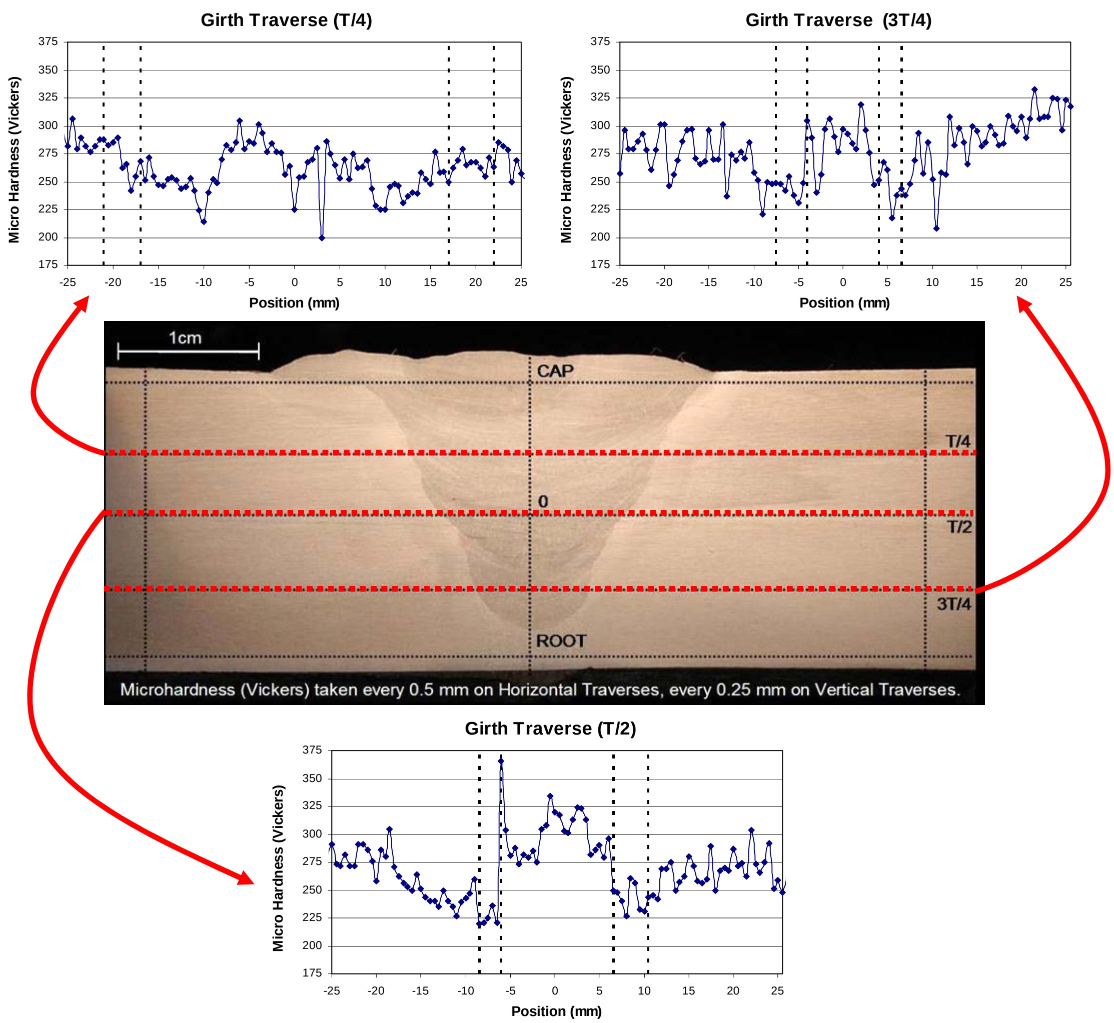

Fig. 5 Girth weld section Vickers micro hardness measurements.

Task 2: Hydrogen charged fatigue crack growth

Influence of Hydrogen on Fatigue Crack Growth: Fatigue tests were performed on compact tension (C(T)) specimens in order to evaluate the influence of hydrogen (H_2) during fatigue crack propagation. The test set-up is shown in Figure 6.

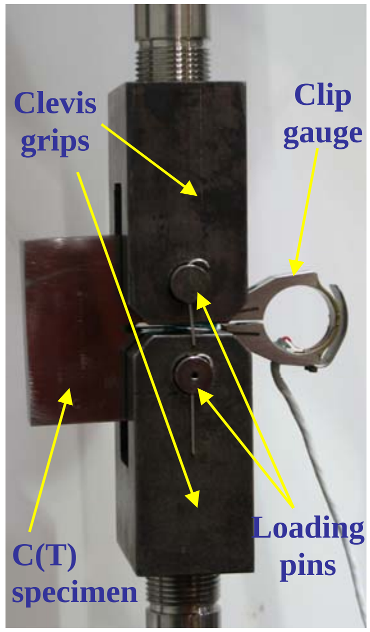

Figure 6. Fatigue experimental set-up.

The tests were performed in air, with hydrogen charging with and without tinning. The samples were charged for 1200 hours (50 days) at 100^{o}C and a pressure of 500 psig. The hydrogen that we achieved was approximately 39 ppm of hydrogen. In order to minimize hydrogen diffusion from the sample, the C(T) specimens were tinned immediately following charging. Figure 7 presents the experimental results.

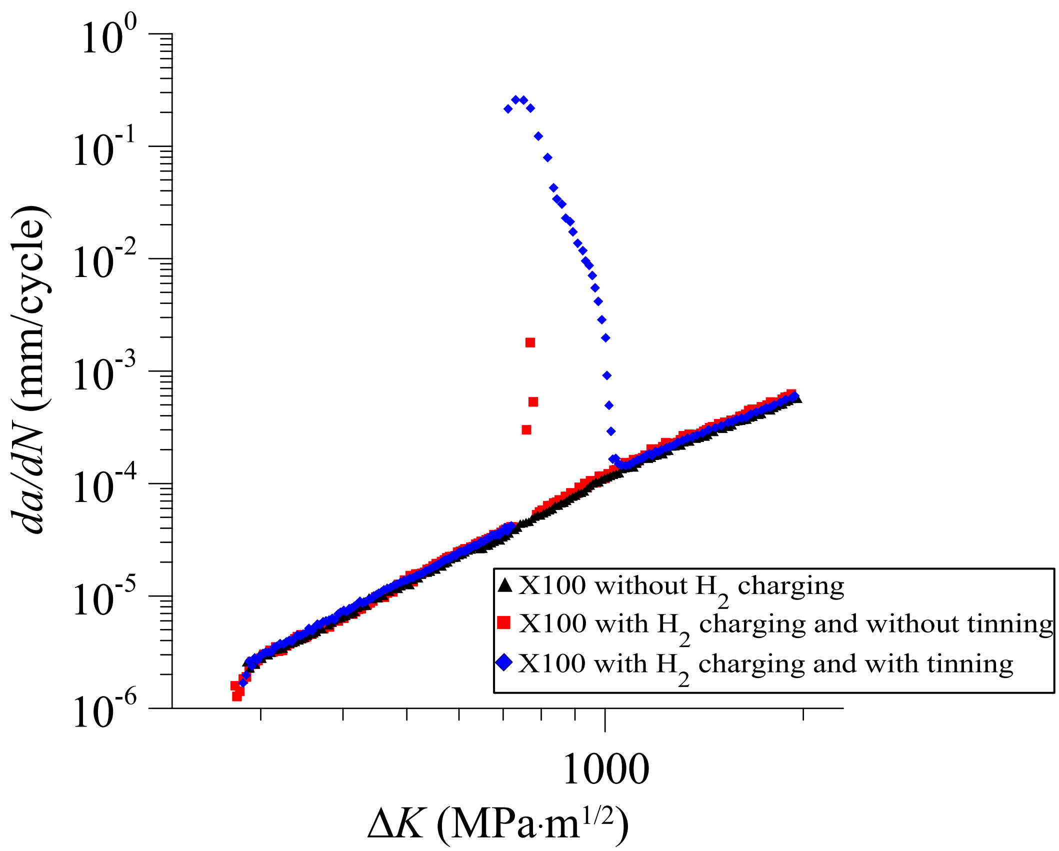

Fig. 7 Experimental results.

The control test (triangle symbol), without hydrogen charging, (but submerged in liquid nitrogen then warmed to room temperature) shows the expected smooth relationship between da/dN and ΔK for the entire test. The second specimen was tested in fatigue for about half its life and followed the same curve. Then, it was charged with hydrogen, and immediately placed in liquid nitrogen until it was returned to the fatigue test machine for further fatigue testing. The crack growth rate (square symbols) immediately jumped by several orders of magnitude, but then returned to the original da/dN versus ΔK relationship after about 15 minutes as the hydrogen diffused from the specimen surfaces. The third specimen (diamond symbol) was precracked the same way, but its surface was tinned (to reduce the loss of hydrogen due to diffusion) immediately after charging. The specimen was then placed in liquid nitrogen until fatigue testing commenced. Its crack growth rate jumped three orders of magnitude for the better part of an hour until it lost the dissolved hydrogen through the fatigue crack surface.

These tests confirm the significant enhancement of fatigue crack growth rate due to dissolved hydrogen. Also, they show the need to perform the tests in a hydrogen environment as even tinned specimens lose hydrogen through the surface of the growing crack.

Task 3: CTOA testing and modeling

CTOA Testing: Quasi-static CTOA testing continues on both girth and seam weld direction fracture specimens. Previous efforts were focused on base metals with cracks oriented in the axial direction. The current effort continues to examine fracture resistance along the girth weld and girth heat affected zone (HAZ) as well as base metal in the girth direction. In addition, seam weld CTOA specimens have been machined to study ductile fracture resistance in the HAZ of the seam weld and weld metal, and specimens have been machined and tested with the crack propagating across the girth weld. Precracking

of the specimens is underway and the CTOA tests should start again early in the next quarter.

Dynamic CTOA Testing: During this quarter, we conducted some relatively high-speed CTOA tests on X65 and X100 pipeline steel using the spring fixture that we assembled during this past quarter (Figure 8). The fixture permitted us to extend the crack velocity to about 6 orders of magnitude higher than the conventional quasi-static procedure.

Figure 8. Spring apparatus for dynamic CTOA testing.

Those preliminary tests were conducted using a high speed camera (up to 40,000 frames/s). The main purpose of these test was to get a better estimation on the crack rate velocity that we can obtain for the steel samples using the spring fixture. A secondary purpose was to check if the camera image resolution was sufficient to capture a picture that can be analyzed to determine the CTOA value.

Initially, we used aluminum samples for setting up the system. However, the aluminum samples created new issues with light reflection and we spent a considerable amount of time correcting for that. Careful adjustment of the lighting and image magnification created images sufficient for analysis.

We are currently precracking X100 and X65 samples for the dynamic test apparatus. We will conduct dynamic tests at various rates and expect to complete the dynamic testing by the end of the next quarter.

Single Edge Notch Tension Testing: The single edge notch tensile [SEN(T)] test provides a measure of fracture toughness with constraints similar to those observed in pipelines during service. This test, as developed by the researchers at SINTEF Materials Technology, will enable us to determine the ductile-to-brittle transition temperature for pipeline material to provide fracture toughness properties for high-strength steel pipeline materials.

At the present time the environmental chamber, in which the low temperature tests (to –80 °C) will be conducted, has been validated. Fixtures for the test have been machined, heat treated where necessary, and assembled. Also four dummy specimens have been machined to use to develop test procedures without loss of essential material. Actual test specimens are in the process of being prepared. The controller for the servo-hydraulic load frame on which the SEN(T) tests will be conducted has been ordered and should arrive within the next two months, at which time the testing will commence.

Modeling:

The CTOA modeling effort described in the last quarterly report continues and will be reported on in the next quarterly report. In addition, Steve Mates and Richard Fields of the NIST Metallurgy Division are continuing their efforts in high strain rate modeling. Their progress follows:

Predicting High Rate Fracture Behavior of Pipeline Steels from Low Rate Fracture Tests and High Rate Plasticity Measurements: This aspect of the program supplements the measurements of CTOA to include effects of rate and temperature on fracture energy. It is well known that the CTOA or CTOD quantifies the kinematic aspects of the ductile fracture process while the rate and temperature behavior of the steel's plasticity control the dynamics. This plasticity can be measured separately from the CTOA or CTOD using the compression Kolsky bar method. Many investigators have shown that the J-integral, the work of fracture, and the dynamic tear energy scale with the product of the flow stress and the CTOD. To date, Kolsky bar tests have been run at room temperature and at -20º C on all the pipeline steels in this program. The room temperature strain rate sensitivity has been determined as well for all these steels. The determination of the strain rate sensitivity at -20º C awaits quasi-static test results that will be available in the next quarter. This data is being used to develop families of stress-strain curves that are functions of strain rate and temperature for all the pipeline steels included in this program. These curves may be combined with the CTOA or CTOD results to predict the generalized strain energy release rate for a propagating crack at any speed and temperature.

Modeling of high speed crack propagation and arrest has focused on combining the high rate plasticity and CTOA to predict large scale behavior. This work has identified two issues. First, while the CTOA is related to the CTOD by simple geometry, in the case of initiation of cracking, it seems that this relation does not work for a moving self similar crack ahead of which the plastic zone has already formed. The CTOD includes a displacement associated with the plastic zone that is not included in the CTOA. Until this issue is cleared up, the CTOD has been evaluated using the thickness reduction (TR). The other issue has to do with thickness effects on CTOA. Fracture test specimens that are thinner than the plastic zone size exhibit a CTOA significantly below that for full thickness plates. Once the thickness approaches and exceeds the plastic zone size, the CTOA tends to plateau. It then gradually decreases to a constant value as plane strain effects and constraint increase. Thus, while thinning of the curved plates to 8 mm in the test section may produce valid CTOAs, thinning to 3 mm results in CTOA's that are lower and not typical of the full thickness pipe plate.

The modeling effort has produced a preliminary report on the prediction of high rate fracture behavior of pipeline steels from low rate fracture tests and high rate plasticity measurements. If the dynamic toughness or fracture energy is normalized by the quasistatic toughness, the effect of strain rate sensitivity on toughness can be seen in Figure 9. The effect of high strain rate sensitivity is to increase the dynamic

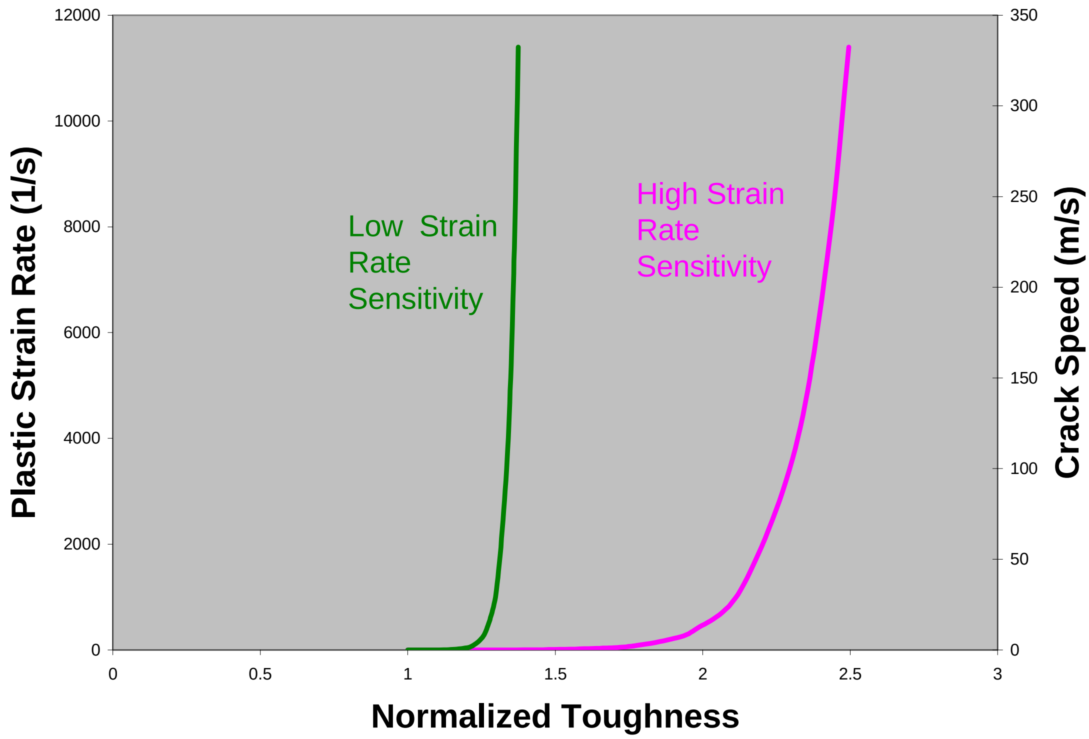

Figure 9. Effect of strain rate sensitivity on normalized toughness as a function of crack speed or plastic strain rate.

toughness by a factor of two or more above the quasistatic toughness at even relatively low speeds. This limits the speed of the crack and may even result in early arrest as the gas decompression wave unloads the pipeline. On the other hand, steels with low strain rate sensitivity have a much lower toughening with crack velocity, can reach very high speeds, and are much less likely to arrest. This shows the importance of having pipeline steels with a relatively high strain rate sensitivity.

Using some of the concepts developed in this report, the drop weight tear test energy of various samples of X100 pipes were predicted using the TR and flow stress, with and without strain rate sensitivity. The results are shown in Figure 10. The predictions using high rate flow stresses are better than the ones using static values, again showing the importance of strain rate sensitivity. Even the predictions using high rate data tend to underestimate the measured values. This is most likely due to the fact that the DWTT's were determined at -18 °C, the temperature at which the large scale test was carried out, while the other data was measured at room temperature. Using flow stresses and strain rate sensitivities for the same temperature as the DWTT's will improve the agreement. This will be carried out in the next quarter.

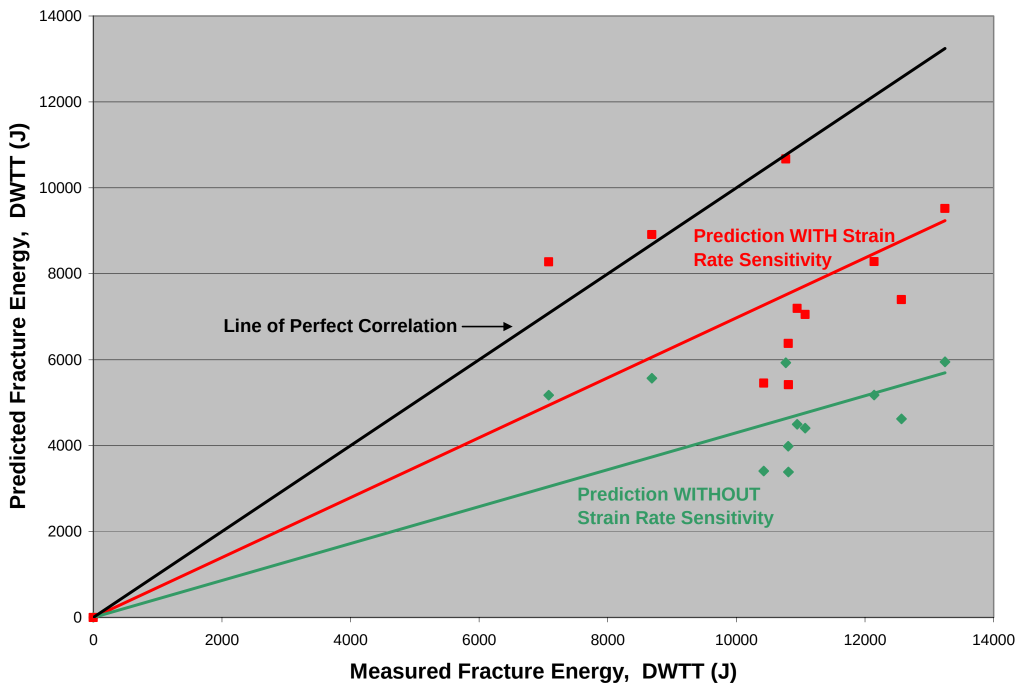

Figure 10. Measured DWTT versus predictions with (dynamic) and without (static) strain rate sensitivity.

Task 4: CTOA Fracture Surface Evaluation

Evaluations of fractured CTOA samples from quasi static tests and dynamic tests show both similarities and differences. For example, the thickness for all of the samples tested were thinned by about 2 to 3 mm (reduction in thickness due to plastic flow), as shown in Figures 11. So, testing rates did not influence thinning appreciably and the finding is similar to the 3 mm of thinning observed for the full scale X100 pipe tested by BP (same X100 material), included in Figure 12. Differences in the distance over which plastic deformation thins the material are apparent in Figure 12. These differences are attributed to constraint of plastic flow due to CTOA sample design.

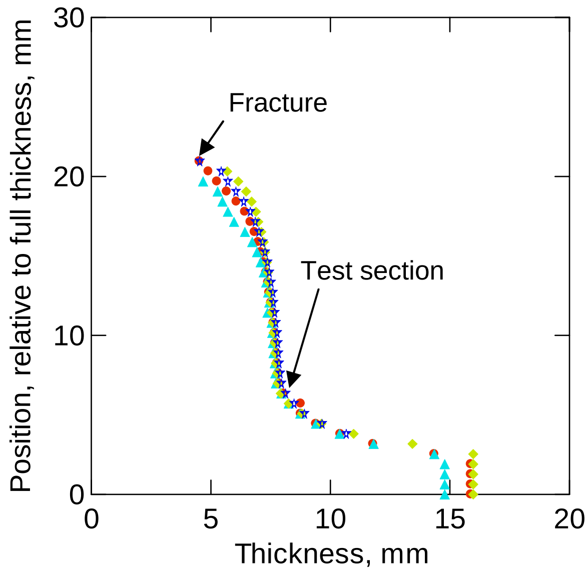

Figure 11: Four X100 CTOA samples, with crack growth rate ranging from about 0.03 mm/s to 5000 mm/s. Note that the test section is 8 mm thick, and is reduced from a thickness of about 15 mm.

The fracture surface features of the CTOA samples also show differences associated with testing rate. Generally the texture associated with the ductile failure surface for the X100 and X65 steels is smoother for tests performed at higher rates. These texture differences are easy to see qualitatively, but difficult to measure.

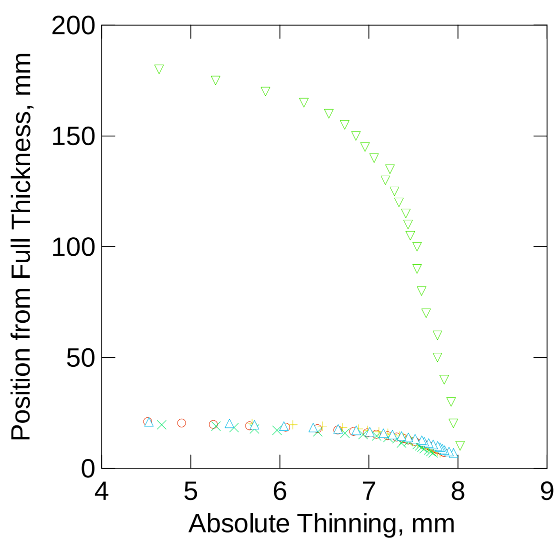

Figure 12: The thinning of the full scale X100 pipe that had been previously explosively tested (with deformation over 150 mm from the fracture location), compared with the 4 CTOA samples in Figure 11 (with deformation over a distance of about 20 mm).

The fracture surface of the X100 steel, unlike the X65 steel, shows markings associated with discontinuous crack growth, Figure 13. At the lower crack growth rates (0.1 mm/second), crack growth is observed to incrementally step forward, then re-blunt slightly prior to the next growth segment. This discontinuous growth process is apparent when the fracture surface markings, shown in Figure 13A, are considered. The small vee-tears mark positions of arrest and re-blunting. CTOA testing planned at intermediate speeds should help define these effects.

CTOA testing is expected to be completed next quarter, and fracture surface evaluations will be conducted on all pertinent specimens. Microscopy from the X65 steels, Figure 14, now being tested show a range in microstrutures from typical ferrite/pearlite banded stuctures, to very uniform fine grained structures. This should provide a good range in properties and fracture appearance for the testing.

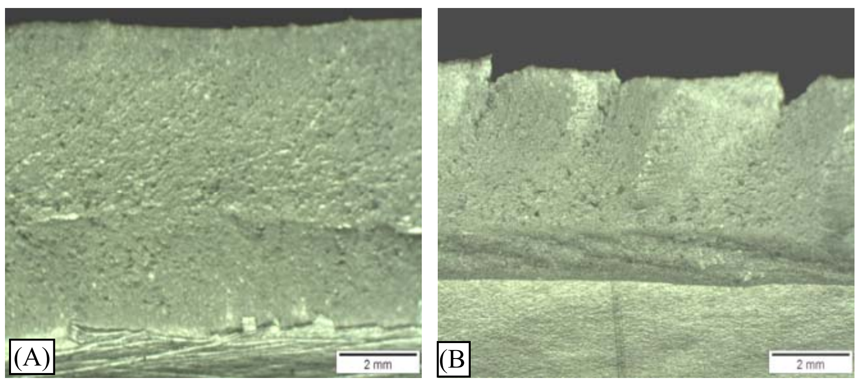

Figure 13: Fracture surfaces of CTOA X100 samples having average crack rates of about (A) 0.1 mm/sec and (B) 5000 mm/sec. At the lower rate there is discontinuous crack grow in the X100 steel, which results in the repeating pattern characteristic of the fracture. The fracture surface of the sample run at higher rates is uniform, indicative of crack growth at a more or less constant speed

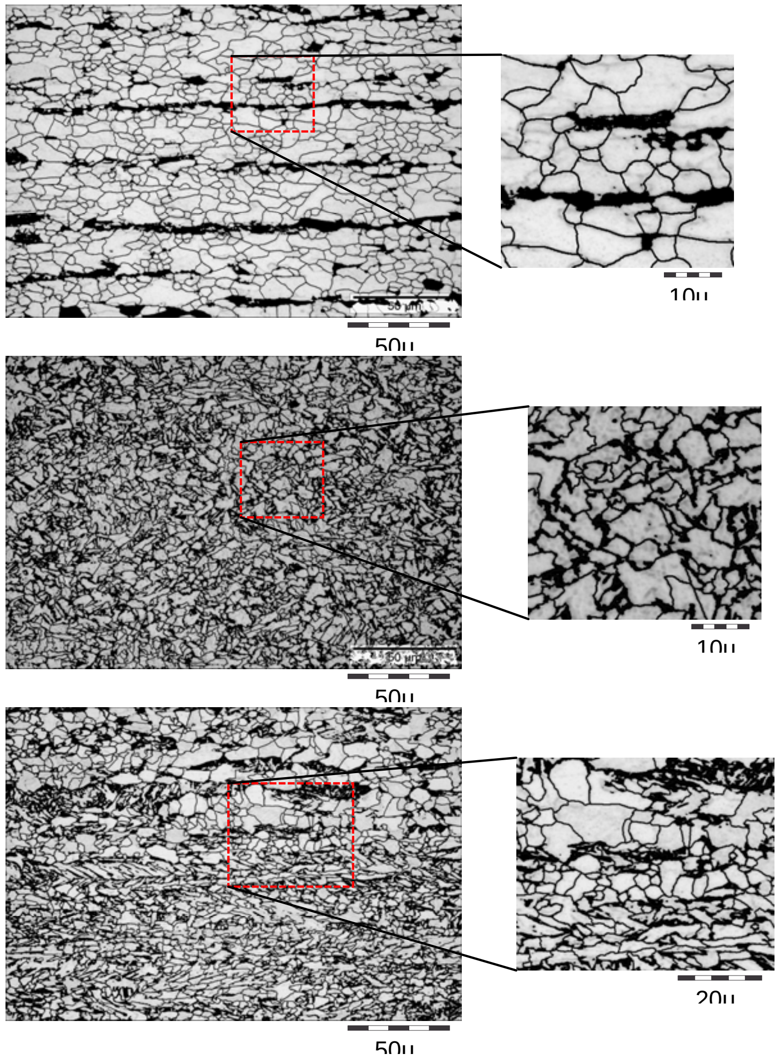

Figure 14: Microstructures of the three X65 pipeline steels.

Task 5: Method for determination of yield strength in high strength pipeline steels and welds

We are initiating a new test program, focusing on the X100 pipeline steels, designed to help us to better understand the yield-strength behavior of these high strength steels. The program will test round tensile specimens that have ¼-, 3/8-, and ½-inch diameter gauge sections. The material will not be flattened to avoid Bauschinger effects. Furthermore, the ¼-inch diameter specimens will originate from the upper and lower half of the through thickness. The test matrix is designed to determine if location and sampling size influence the yield strength. Material from two X100 sources will be tested for comparison. At this time, the material has been sent for machining, and testing should commence before the end of this quarter.

Task 6: Other tasks

In addition to supporting this effort through laboratory research, NIST representatives have attended PSIA meetings, reviewed proposals and peer-reviewed projects as needed. A presentation given on our CTOA efforts to ASTM Committee E08 on Fracture Mechanics. Reports published or submitted for publication, conferences attended and symposia participation follows:

Papers and conferences this reporting quarter:

Crack Tip Opening Angle Optical Measurement Methods in Five Pipeline Steels
Ph. P. Darcis, C. N. McCowan, H. Windhoff, J. D. McColskey and T. A. Siewert
Engineering Fracture Mechanics, *September 2007.*

Conferences

Fracture Toughness through a Welded Pipeline Section - Crack Tip Opening Angle Criterion -
Ph. P. Darcis, C. N. McCowan, E. S. Drexler, J. D. McColskey, A. Shtechman and T. A. Siewert
International IIW conference Welding & Materials Technical, economic and ecological aspects, Cavtat & Dubrovnik, Croatia, July 05-06, 2007.
.

Reporting
This is the fifth quarterly report under agreement number DTPH56-06-X-000029. The next quarterly report will be submitted in 3 months.